Reports

Intensity Dependence of the Fluorescence Lifetime of in vivo Chlorophyll Excited by a Picosecond Light Pulse

Abstract. *New data on intensity-dependent lifetimes indicate that all previous in vivo fluorescence studies of chlorophyll by picosecond techniques must be reinterpreted. Anomalously short lifetimes result from high-intensity effects due to exciton-exciton annihilation processes. Measurements in* Chlorella pyrenoidosa *with single-pulse, low-intensity excitation indicate a longer "true" lifetime of 650 ± 150 picoseconds.*

We recently investigated the in vivo fluorescence yield of chlorophyll excited with a single 530-nm light pulse 20 psec in duration (*1*). On the basis of previously reported "single-pulse" quantum efficiency measurements and new lifetime data presented here, we conclude that there is an alternative interpretation for all previous in vivo chlorophyll fluorescence results obtained by picosecond techniques. Previous studies (*2–9*) involved the use of high-intensity ultrashort pulses from mode-locked lasers in conjunction with optical gate (*2–4*) or streak camera (*5–9*) detection. The observed lifetimes were considerably shorter than those previously obtained with nanosecond flashes (*10–14*) or those estimated on the basis of quantum efficiencies (*15, 16*). As these measurements are essential for understanding efficient energy migration processes of photosynthesis, it is important to interpret this anomaly. We have proposed (*1*) that the short lifetimes result from the use of a very high intensity mode-locked laser pulse train as an excitation source and subsequent exciton-exciton annihilation processes occurring within the photosynthetic unit (PSU). Beddard *et al.* (*9*) also considered the possibility of such annihilative collision processes, but arrived at the opposite conclusion. We believe this controversy can be resolved with the new lifetime data presented here. We demonstrate that variations in the lifetime with excitation intensity are readily observed in single-pulse experiments and arise from the exciton-exciton annihilation processes within the PSU. We further determine that under single-pulse, low-intensity excitation the in vivo chlorophyll a fluorescence decay time for *Chlorella pyrenoidosa* is 650 ± 150 psec, a much longer lifetime than previously reported for this species with picosecond techniques (*5, 6, 9*), but in agreement with earlier low-intensity measurements (*10–12*).

Using a single pulse selected from a mode-locked Nd:YAG (Nd^{3+}:yttrium aluminum garnet) laser by means of a longitudinal-mode potassium dihydrogen phosphate (KDP) Pockels cell (*17*) and doubling its frequency in KDP, we excited samples of *C. pyrenoidosa* with a 20-psec pulse of 530-nm light. The 530-nm pulse is propagated over a long delay path to the sample, allowing diffraction to smooth spatial inhomogeneities. The beam expands to a diameter of 9 mm, and is truncated to a known diameter with uniform intensity across its radial profile by a 3-mm aperture placed on axis. A lens images this desired profile onto the *C. pyrenoidosa* sample cuvette. A beam-splitting mirror after the aperture directs a portion of the pulse to a Laser Precision energy meter. Since the radial profile is accurately known, the beam intensity for each shot can be calculated. The resulting fluorescence at 700 nm was observed from the front of the cuvette using an S-20 Electro-Photonics streak camera with modified *f*/1 optics. An SSR 500-channel silicon vidicon optical multichannel analyzer (OMA) was coupled through a lens to the streak camera so that the fluorescent streak could be conveniently displayed on an oscilloscope or chart recorder. The lifetimes reported here were calculated directly from the OMA's digital readout. Calibration has shown that the device is nearly linear over a range of 700. The excitation intensity required for recording is a function of the fluorescing sample, streak rate, optics, and slit width. With modified input optics and optimum coupling fluorescence from *C. pyrenoidosa* is recorded with a single 1-μj excitation pulse at 3×10^{14} photon/cm^2; the time resolution (20 psec) is limited by the laser pulse duration. By increasing the input slit width of the streak camera the sensitivity can be increased, but at the expense of resolution. The sample, *C. pyrenoidosa* (Sorokin's strain ICC No. 1230), was prepared as described in (*6*).

Fluorescence from *C. pyrenoidosa* is shown in Fig. 1, A to C. The excitation intensities are, respectively, 10^{14}, 3×10^{14}, and 3×10^{15} photon/cm^2. The fluorescence in these cases decays to the 1/*e* point in 375 ± 50, 175 ± 25, and 50 ± 10 psec, respectively. In Fig. 1, A and B, the streak camera slits were opened by a factor of 2 for increased sensitivity (temporal resolution ≈ 30 psec). Taking into account the relative slit widths, the relative peak amplitudes were determined to be 1.0, 2.6, and 20, respectively. It is probable that in Fig. 1C the initial ultrafast decay is not fully resolved. All curves shown are nonexponential, and consequently the 1/*e* point given here has no special significance other than as a measure of the rapid variation of the decay with intensity. A weak component of fluorescence with a decay time of 1.5 nsec is also present.

Previous picosecond experiments involved excitation intensities that were typically in the range 0.1 to 10 mj/cm^2 (3×10^{14} to 3×10^{16} photon/cm^2 at 530 nm). In *C. pyrenoidosa* the total cross section for absorption of the PSU is thought to be of the order of 100 Å^2 at 530 nm (*18*), so that at the intensities found in these experiments the PSU is multiply excited. Under these conditions there is a high probability that two or more singlet excitons might interact and cause a decrease in both the observed fluorescence lifetime and the quantum efficiency. Further complications arise because of the use of a train of mode-locked pulses. In experiments with the optical gate (*2–4*) data are typically accumulated from all of the pulses in the train, while in those with streak cameras (*5–9*) fluorescence from a single pulse near the center of the train is typically examined. As these trains consist of about 100 high-intensity pulses, pulses exciting the sample before the pulse chosen for streak camera investigation may populate the reaction centers, leave a residual population of antenna chlorophyll molecules in the triplet state, or otherwise

change the system. Thereafter, singlets generated by the pulse to be examined interact with the altered system.

The strongest evidence against these effects was the linear proportionality of fluorescence with intensity observed by Seibert *et al.* (*2*, *3*). Beddard *et al.* (*9*) further showed that with pulse train excitation the fluorescence lifetime was constant over a decade variation in excitation intensity, an experimental observation verified by us independently (*19*). Nevertheless, a reinvestigation of this point was prompted by the recent results of Mauzerall (*18*), who showed that the quantum efficiency of fluorescence emission from *C. pyrenoidosa* decreases at high pumping intensities for 7-nsec excitation pulses and interpreted the decrease in terms of a multitrap model of the PSU and exciton-exciton collisions. Consequently, Campillo *et al.* (*1*) repeated these quantum efficiency measurements with a single pulse selected from a mode-locked Nd:YAG laser at intensities comparable to those in the previous picosecond measurements. The results showed a decrease in quantum efficiency with intensity, in agreement with the results of Mauzerall. The relative quantum efficiency $\phi(I)/\phi_0$ (the quantum efficiency at intensity I divided by the quantum efficiency at low intensity) was observed to decrease at an energy density of 10^{13} photon/cm^2, reaching values of 0.8 at 6×10^{13} photon/cm^2, 0.6 at 3×10^{14} photon/cm^2, 0.4 at 10^{15} photon/cm^2, and 0.2 at 2×10^{16} photon/cm^2. The functional form of this decrease is most interesting and is consistent with singlet-singlet annihilation processes according to the theoretical considerations of Mauzerall (*18*), Goad and Gutschick (*20*), and Swenberg *et al.* (*21*).

For single picosecond pulse excitation, bimolecular processes other than singlet-singlet annihilation appear to be unlikely. Singlet-triplet (*22*) annihilation should play no role because of the long time for triplet formation, while interaction of singlets with charge states in the reaction center can be ruled out by recent experiments that show similar effects in chromatophores without reaction centers (*23*). It is important to note here that the manner in which the excitons interact strongly reflects the network of chlorophyll-chlorophyll interactions within the PSU. Attempts (*18*, *20*, *21*) have therefore been made to fit the observed data to gain new insight into the topology of *C. pyrenoidosa*. Researchers have used a Stern-Volmer equation approach with a term, $-\gamma_{ss}n_s^2$, added to reflect the singlet exciton annihilation processes (γ_{ss} is a bimolecular rate constant for singlet-singlet annihilation and n_s is the singlet excited state population, which is proportional to the observed fluorescence), and have averaged over independent PSU's with a Poisson distribution of multiple excitations to show that a slow decrease in quantum efficiency with increasing intensity is to be expected. It is important not to experimentally introduce additional effects that might cloud the data, such as nonuniform excitation. Since there is excellent penetration of the *C. pyrenoidosa* lamellar substructure at an excitation wavelength of 530 nm because chlorophyll a and chlorophyll b absorb poorly there, induced gradients in the absorption causing a shading effect are avoided.

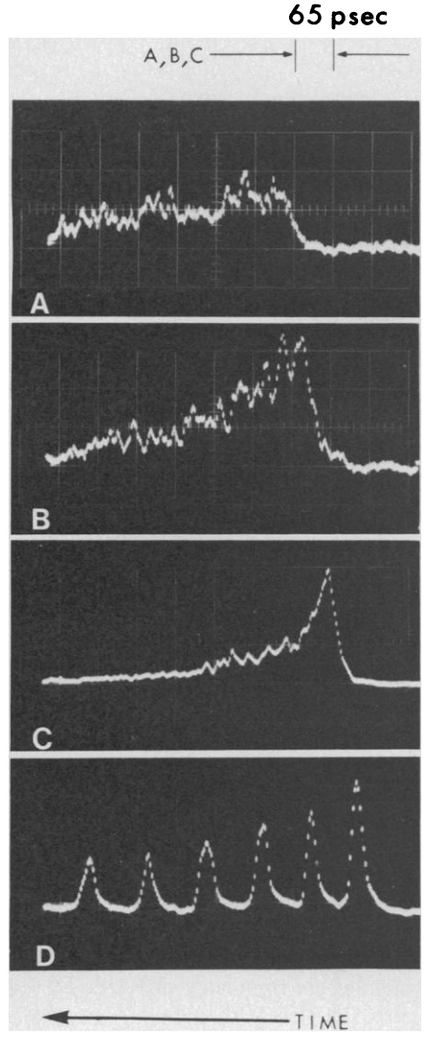

Fig. 1. OMA-oscilloscope displays of 700-nm fluorescent streaks from *C. pyrenoidosa* excited with a single 20-psec, 530-nm pulse. Excitation intensities are (A) 10^{14}, (B) 3×10^{14}, and (C) $\simeq 3 \times 10^{15}$ photon/cm^2. The measured 1/*e* points are (A) 375, (B) 175, and (C) <50 psec. The relative peak intensities were (A) 54, (B) 141, and (C) 540 counts, with a slit width setting in (C) of half that used in (A) and (B); see text. This variation in fluorescence lifetime with intensity is consistent with singlet-singlet exciton processes occurring within the photosynthetic unit. (D) Train of calibration pulses generated by passing a single 530-nm pulse through two parallel mirrors (reflectivity = 92 percent at 530 nm). The resulting train has a known exponentially decaying envelope function and can be used to calibrate the apparatus. Neutral density filters can be inserted between the mirrors or the mirror separation can be varied to alter the envelope decay rate. Using this scheme, we could verify that the OMA–streak camera response and streak rate were linear. The streak rate in (D), 115 psec per major division, was somewhat slower than that in (A) to (C) in order to display more of the pulses in the calibration train. The width of the pulses shown in (D) is limited by the resolution of the instrument at this streak rate. Observations of a single 530-nm pulse at the streak rate of (A) to (C) show that the width of the 530-nm pulse is 20 psec.

The variation in fluorescence decay time with intensity reported here is, we believe, consistent with singlet-singlet annihilation. A Stern-Volmer equation describing such a process is simply written, $dn_s/dt = -kn_s - \gamma_{ss}n_s^2$, valid for time $t > 20$ psec. Here k is a characteristic decay rate constant related to trapping, intersystem crossing, and radiative losses ($k = 1/\tau$, where τ is the fluorescence lifetime). The solution for n_s is nonexponential (*21*); however, the initial decay rate can be estimated from the Hartree approximation (*24*) $dn_s/dt \approx -kn_s - (\gamma_{ss}\bar{n}_s)n_s$, where $\bar{n}_s$ is the initial density of excited states. Thus, the initial decay rate observed with a streak camera technique is $K_{obs} \approx k + \gamma_{ss}\bar{n}_s$. To estimate γ_{ss} one must have specific information on the PSU geometry, such as dimensionality. It is convenient to define $\Gamma \equiv \gamma_{ss}\bar{n}_s/I$, where Γ is independent of PSU geometry. With this simple formulation we obtain a reasonable fit to our data. We find that $\Gamma \simeq 1.5 \times 10^{-5}$ cm^2 photon^{-1} sec^{-1} and $k = 1.25 \times 10^9$ sec^{-1}, and hence $\tau \approx 800$ psec. An alternate approach in estimating τ involves using both streak camera data and the observed quantum efficiencies reported in (*1*). We assume that the relationship $\tau \approx \tau(I)/[\phi(I)/\phi_0]$ is valid at intensities $< 10^{14}$ photon/cm^2. Using this approach, we estimate $\tau \approx 535$ psec. We suspect that the Hartree approximation yields an estimate that is high because it neglects the presence of a distribution of multiple excitations within the individual independent PSU's. The quantum efficiency approach is suspected to give a low estimate because of background radiation. Nevertheless, an average of these two approaches yields $\tau \approx 650 \pm 150$ psec. This value agrees well with earlier low-intensity measurements (*9*–*11*) and those estimated using quantum efficiencies (*14*,

15), but is much longer than values found in previous picosecond studies. This measurement of τ should at some time in the future be performed at intensities below 10^{13} photon/cm^2. This is at present beyond the capabilities of our apparatus.

As previous picosecond studies involved excitation intensities exceeding 10^{14} photon/cm^2 [for example, Beddard *et al.* (*9, 25*) used $I > 10^{15}$ photon/cm^2 and Yu *et al.* (*4*) and Seibert and Alfano (*3*) used $I > 6 \times 10^{14}$ photon/cm^2], the data obtained must also reflect exciton annihilative processes. We believe the observations in (*2–9*) can be explained by their use of full mode-locked pulse trains and by a singlet-triplet annihilation process. Triplets, which evolve from singlets by intersystem crossing, live longer [τ_T = 30 nsec in vivo (*26*)] than the time interval between pulses in the train [Δt = 6.7 nsec (*9*)]. Thus, the triplet population will increase from pulse to pulse until a steady-state value, N_{Tss}, is established. This value is limited at high intensities through a combination of singlet-singlet and singlet-triplet annihilation processes, eventually becoming independent of I. In this "saturated" regime, an appropriate Stern-Volmer equation for n_s is simply expressed as $dn_s/dt = -\gamma_{ST}N_{Tss}n_s$ and has a nearly exponential decay rate, $\gamma_{ST}N_{Tss}$, independent of I. This picture is similar to the observations in (*5, 6, 9*). The singlet state decay constant, $\gamma_{ST}N_{Tss}$, is observed to be in the range 10^{10} to 3×10^{10} sec^{-1}. Certainly these annihilation processes must occur at these intensities, and we suggest this an an alternative interpretation to the previous experimental observations.

A. J. CAMPILLO
V. H. KOLLMAN
S. L. SHAPIRO

University of California,
Los Alamos Scientific Laboratory,
Los Alamos, New Mexico 87545

References and Notes

1. A. J. Campillo, S. L. Shapiro, V. H. Kollman, K. R. Winn, R. C. Hyer, *Biophys. J.* **16**, 93 (1976).
2. M. Seibert, R. R. Alfano, S. L. Shapiro, *Biochim. Biophys. Acta* **292**, 493 (1973).
3. M. Seibert and R. R. Alfano, *Biophys. J.* **14**, 269 (1974).
4. W. Yu, P. P. Ho, R. R. Alfano, M. Seibert, *Biochim. Biophys. Acta* **387**, 159 (1975).
5. V. H. Kollman, S. L. Shapiro, A. J. Campillo, *Biochem. Biophys. Res. Commun.* **63**, 917 (1975).
6. S. L. Shapiro, V. H. Kollman, A. J. Campillo, *FEBS Lett.* **54**, 358 (1975).
7. V. Z. Paschenko, A. B. Rubin, L. B. Rubin, *Kvantovaya Elektron. (Moscow)* **2**, 1336 (1975).
8. V. Z. Paschenko, S. P. Protasov, A. B. Rubin, K. N. Timofeev, L. M. Zamazova, L. B. Rubin, *Biochim. Biophys. Acta* **408**, 143 (1975).
9. G. S. Beddard, G. Porter, C. J. Tredwell, J. Barber, *Nature (London)* **258**, 166 (1975).
10. W. J. Nicholson and J. I. Fortoul, *Biochim. Biophys. Acta* **143**, 577 (1967).
11. A. Müller, R. Lumry, M. S. Walker, *Photochem. Photobiol.* **9**, 113 (1969).
12. G. S. Singhal and E. Rabinowitch, *Biophys. J.* **9**, 586 (1969).
13. H. Merkelo, S. R. Hartman, T. Mar, G. S. Singhal, Govindjee, *Science* **164**, 301 (1969).
14. A. Yu. Borisov and V. I. Godik, *Bioenergetics* **3**, 211 (1972).
15. N. R. Murty, C. N. Cederstrand, E. Rabinowitch, *Photochem. Photobiol.* **4**, 917 (1965).
16. P. Latimer, T. T. Bannister, E. Rabinowitch, *Science* **124**, 585 (1956); in *Research in Photosynthesis*, H. Gaffron, Ed. (Interscience, New York, 1957), p. 107.
17. R. C. Hyer, H. D. Sutphin, K. R. Winn, *Rev. Sci. Instrum.* **46**, 1333 (1975).
18. D. Mauzerall, *Biophys. J.* **16**, 87 (1976).
19. A. J. Campillo, V. H. Kollman, S. L. Shapiro, unpublished results.
20. W. B. Goad and V. Gutschick, in preparation.
21. C. Swenberg, N. Geacintov, M. Pope, in preparation.
22. T. S. Rahman and R. S. Knox, *Phys. Status Solidi (b)* **58**, 715 (1973).
23. A. J. Campillo, T. G. Monger, W. W. Parson, S. L. Shapiro, in preparation.
24. Suggested by C. E. Swenberg, private communication.
25. J. Barber, private communication.
26. J. Breton and P. Mathis, *C. R. Acad. Sci.* **271**, 1094 (1970).
27. Supported by the Energy Research and Development Administration. We thank W. B. Goad, D. Mauzerall, and C. E. Swenberg for helpful discussions and R. C. Hyer and K. R. Winn for experimental assistance.

23 January 1976; revised 14 April 1976

Effect of Infrared Transparency on the Heat Transfer Through Windows: A Clarification of the Greenhouse Effect

Abstract. *The various radiative, convective, and conductive components of the net heat transfer are calculated and illustrated for various infrared transparencies of covers such as would be used in architectural, greenhouse, or solar collector windows. It is shown that in the limiting cases of infrared opacity and infrared transparency the relative contributions of the three modes of heat transfer are altered, but all contribute significantly. The radiation shielding arguments pertain to the analogous greenhouse effect in the atmosphere.*

A number of letters have recently appeared dealing with the interpretation of the greenhouse effect (*1, 2*) and the etymology of the term (*3*). Fleagle and Businger (*1*) and Schwiesow (*2*) state that the infrared (IR) absorption by glass of the room temperature thermal radiation spectrum does little to alter the heat transfer characteristics of terrestrial greenhouses, and hence the thermal losses are essentially all due to convection. These authors cite the early work of R. W. Wood (1909), who "found that two model greenhouses, one covered with glass and the other with rock salt (which is transparent to both short- and long-wavelength radiation) reached very nearly the same high temperature" (*1*). They conclude that the greenhouse effect is due to the suppression of vertical convection by a rigid lid. The implication is that radiative transfer plays a minor role in the terrestrial greenhouse effect.

Indeed, a misconception exists because radiative transfer from the interior of a room, or from a nonevacuated flat plate solar collector to the covering glass window, is at least as important as convective transfer. The physical phenomenon involved, which explains Wood's original observations, is that the sum of the convective and radiative losses is not changed appreciably by going from an IR-opaque cover (glass) to an IR-transparent cover (rock salt or polyethylene). However, the mix of the two contributions on the interior and exterior surfaces of the window is changed. This is illustrated in Fig. 1 for the cases of vertical windows and horizontal skylights. These two cases differ by the nature of the free convective heat transfer coefficient at the interior surface of the window, and also by the effective sky temperature (*4–6*) as seen by windows in different orientations. The convection at the external surface is dominated by forced convection due to wind. The external convective heat transfer coefficient is the same for both orientations. For the example illustrated in Fig. 1, we have chosen the interior temperature as 21°C, the exterior temperature as 0°C, and the wind velocity as 5.36 m/sec. The effective sky radiation transfer temperatures, which depend on atmospheric conditions, are taken as −4.2° and −12°C below the ambient temperature for the vertical and horizontal surfaces, respectively. All units for heat transfer are watts per square meter.

Table 1 shows the mix of the different contributions to the heat transfer for different effective sky radiation temperatures. The sky temperature groupings are −11.4°, −4°C; −4.2°, −12°C; and −7°, −20°C for the vertical and horizontal windows, respectively, under different atmospheric conditions (*4*) for an exterior ambient temperature of 0°C. Figure 1 represents one of the examples in Table 1. The calculational methods used to arrive at these results are outlined at the end of the text.

In the results, the IR-opaque glass windows have higher temperatures than IR-